HHS Public Access

Author manuscript

Am J Transplant. Author manuscript; available in PMC 2020 March 01.

Published in final edited form as:

Am J Transplant. 2019 March ; 19(3): 646–661. doi:10.1111/ajt.15083.

mTORC2 deficiency in cutaneous dendritic cells potentiates CD8+ effector T cell responses and accelerates skin graft rejection

Alicia R. Watson[1,2], **Helong Dai**[1,3], **Julio A. Diaz-Perez**[4], **Meaghan E. Killeen**[4], **Alicia R. Mathers**[4,5], and **Angus W. Thomson**[1,5,*]

[1]Starzl Transplantation Institute, Department of Surgery, University of Pittsburgh School of Medicine, Pittsburgh, PA 15213, USA

[2]Department of Pathology, University of Pittsburgh School of Medicine, Pittsburgh, PA 15213, USA

[3]Department of Urological Organ Transplantation, The Second Xiangya Hospital of Central South University, Changsha, China

[4]Department of Dermatology, University of Pittsburgh School of Medicine, Pittsburgh, PA 15213, USA

[5]Department of Immunology, University of Pittsburgh School of Medicine, Pittsburgh, PA 15213, USA

Abstract

Mechanistic target of rapamycin (mTOR) complexes (C) 1 and 2 regulate the differentiation and function of immune cells. While inhibition of mTORC1 antagonizes dendritic cell (DC) differentiation and suppresses graft rejection, the role of mTORC2 in DC in determining host responses to transplanted tissue remains undefined. Utilizing a mouse model in which mTORC2 was deleted specifically in CD11c$^+$ DC (TORC2$^{DC-/-}$), we show that transplantation of minor histocompatibility antigen (HY)-mismatched skin grafts from TORC2$^{DC-/-}$ donors into wild-type recipients, results in accelerated rejection characterized by enhanced CD8$^+$ T cell responses in the graft and regional lymphoid tissue. Similar enhancement of CD8$^+$ effector T cell responses was observed in MHC-mismatched recipients of TORC2$^{DC-/-}$ grafts. Augmented CD8$^+$ T cell responses were also observed in a delayed-type hypersensitivity model in which mTORC2 was absent in cutaneous DC. These elevated responses could be ascribed to an increased T cell stimulatory phenotype of TORC2$^{DC-/-}$ and not to enhanced lymph node homing of the cells. In contrast, rejection of ovalbumin transgenic skin grafts in TORC2$^{DC-/-}$ recipients was unaffected. These findings suggest that mTORC2 in skin DC restrains effector CD8$^+$ T cell responses and

*Correspondence: Angus W. Thomson, PhD, DSc, Starzl Transplantation Institute, University of Pittsburgh School of Medicine, 200 Lothrop Street, BST W1540, Pittsburgh, PA 15261, thomsonaw@upmc.edu, (412) 624-6392.

AUTHOR CONTRIBUTIONS

A.R.W.: study design, data generation and analysis, and writing of the manuscript. H.D.: data generation and manuscript review. J.A.D-P: data generation, contribution to discussion. M.E.K.: data generation. A.R.M.: study design, contribution to discussion, manuscript review. A.W.T.: research design, analysis of data, writing of the manuscript

DISCLOSURE

The authors of this manuscript have no conflicts of interest to disclose as described by the *American Journal of Transplantation*.

have implications for understanding of the influence of mTOR inhibitors that target mTORC2 in transplantation.

1. INTRODUCTION

The immunosuppressant pro-drug rapamycin is an allosteric inhibitor of the mechanistic target of rapamycin (mTOR), a nutrient sensor[1] with serine-threonine kinase activity that regulates cell growth, metabolism and proliferation[2, 3], as well as immune cell differentiation and function[4–6]. mTOR functions in two distinct complexes: mTOR complex (C) 1 and mTORC2[7]. Assembled mTORC1 phosphorylates and activates the translational proteins ribosomal S6 kinase β−1 (S6K1) and eukaryotic translation initiation factor 4E-binding protein 1 (4E-BP1) and regulates cellular processes in a nutrient-dependent fashion[8]. Conversely, mTORC2 phosphorylates and activates Akt (protein kinase B), protein kinase C and serum and glucocorticoid-regulated kinase 1 and regulates actin cytoskeletal dynamics in fibroblasts[9].

While canonically, rapamycin has been described as a complete and specific mTORC1 inhibitor, work by our group and others has revealed that rapamycin administration may also inhibit mTORC2 activity[10–13]. Indeed, the development of glucose intolerance and insulin resistance in transplant patients receiving rapamycin may be mediated by mTORC2 inhibition[11]. In mice, dual inhibition of mTORC1 and 2 using novel adenosine triphosphase (ATP) competitive inhibitors is less effective in prolonging heart allograft survival than immune suppression with rapamycin alone[14, 15]. However, although selective mTORC2 targeting has been shown recently to block tumor growth in mice[16, 17], we are not aware of any reports of selective mTORC2 targeting in graft donors or recipients.

There is evidence that mTOR controls T helper (Th) Th cell differentiation through selective activation of signaling by mTORC1 and mTORC2[18], that mTORC1 and mTORC2 selectively regulate $CD8^+$ T cell differentiation[19] and that mTORC2 controls $CD8^+$ T cell memory differentiation[20]. While it has been reported that selective mTORC1 disruption in mouse peritoneal macrophages reduces inflammation[21] and that mTORC1 deficiency in intestinal dendritic cells (DC) enhances CD86 expression and suppresses IL-10 production[22], we have shown[23] that deletion of mTORC2 in bone marrow (BM)-derived DC leads to an enhanced pro-inflammatory phenotype. These DC lacking mTORC2 promote allogeneic Th1/Th17 polarization and proliferation in vitro, as well as augmented antigen (Ag)-specific Th1/Th17 responses in vivo[23]. However, how the absence of mTORC2 activity specifically in DC might impact their function, host T cell responses and graft survival in transplant recipients has not been investigated.

To address these questions, we utilized mice in which Rictor, an essential component of mTORC2[9], was knocked out specifically in conventional $CD11c^+$DC ($TORC2^{DC-/-}$)[12] as donors of either non-MHC (minor H-Y) Ag-mismatched or MHC-mismatched skin grafts. Skin grafts were also transplanted from donors expressing transgenic (tg) ovalbumin (OVA) functioning as a minor H Ag onto $TORC2^{DC-/-}$ recipients. Further insight into the role of mTORC2 in skin-resident DC was gained using a cell-mediated, cutaneous delayed-type

hypersensitivity (DTH) model. Our novel findings identify mTORC2 in cutaneous DC as a negative regulator of $CD8^+$ effector T cell responses and skin graft rejection.

2. MATERIALS AND METHODS

2.1. Mice

Male and female C57BL/6 (B6; $H2^b$) CD11c-$CreRictor^{f/f}$ (herein referred to as $TORC2^{DC-/-}$) mice were generated as described[12]. CD11c-Cre- littermates were used as negative controls. C57BL/6-Tg(CAG-OVA)916Jen/J (herein referred to as OVA^+) mice were generously provided by Drs. D. Rothstein and F. Lakkis (University of Pittsburgh). Female BALB/cByJ (BALB/c) mice were purchased from The Jackson Laboratory. All studies were performed according to an Institutional Animal Care and Use Committee-approved protocol in accordance with NIH guidelines.

2.2. Skin transplantation, graft assessment and Banff scoring

Skin transplantation was performed as described by Billingham et al[24], with some modifications [25]. Banff rejection scores were determined by a 'blinded' dermatopathologist (J.A.D.-P) based on established criteria [26, 27].

2.4. Graft immunohistochemistry

Skin grafts were harvested and fixed for 24 hours in 4% v/v paraformaldehyde (PFA). H&E, CD3 (Abcam; Cambridge, MA; clone # ab16669), CD4 (Abcam; ab183685) and Alcian blue staining was performed and quantitative analysis of immunohistochemical staining performed using the FIJI ImageJ IHC Toolbox plug-in (NIH).

2.5. Graft recipient T cell analysis

T cells isolated from graft-draining axillary lymph nodes (LN) via negative immunomagnetic bead selection were either (1), analyzed via flow cytometry following surface staining with monoclonal antibody (mAb) against CD3 (eBioscience, Waltham, MA; clone# 17A2), CD4 (eBioscience; RM4–5), CD8 (eBioscience; 2.43), PD-1 (eBioscience; J105) and intracellular staining for Foxp3 (BioLegend, San Diego, CA; FJK-16s) or (2), labeled with carboxyfluorescein succinimidyl ester (CellTrace CFSE) according to the manufacturer's instructions (Invitrogen; Carlsbad, CA) and co-cultured with splenic DC (1 DC:10 T cells) isolated via immunomagnetic bead selection from donor-matched mice (male B6, female B6 or OVAtg) that had been injected i.p. with 10μg of fms-like tyrosine kinase 3 ligand per day for 10 days before DC isolation[28]. After 3 days of culture, IFNγ, IL-2, IL-4, and Granzyme-B (GrB) levels in supernatants were determined by enzyme-linked immunosorbent assay (ELISA) as per the manufacturer's instructions (BioLegend or eBioscience [GrB]). Leukocytes isolated from grafts following collagenase digestion as described[29] were preincubated with Mouse BD Fc Block purified anti-mouse CD16/CD32 mAb (BD Biosciences; clone# 2.4G2) for 5 min on ice followed by viability staining (Zombie Aqua Fixable Viability Kit 423101, BioLegend) and surface staining for CD45.2 (eBioscience; clone# 104), CD3 (eBioscience; 17A2), CD4 (eBioscience; RM4–5), CD8 (eBioscience; 2.43) and programed death-1 (PD-1; eBioscience; J105). Flow data were

acquired using a Fortessa flow cytometer (BD Biosciences, San Jose, CA) and analyzed using FlowJo (Tree Star, Ashland, OR).

2.6. Delayed-type hypersensitivity (DTH) responses

Cutaneous DTH reactions to 1-Fluoro-2,4-dinitrobenzene (DNFB) were induced and elicited (in ear pinnae) as described[30] with minor modifications[31] and quantified using an electronic caliper (Mitutoya 700–118-20, Aurora, IL).

2.7. Immunofluorescence staining of tissue sections

DNFB-challenged and control ear pinnae were obtained 72 hours post-challenge, flash-frozen and embedded in OCT compound. Cryostat sections (7μm) were fixed in 4% v/v PFA at room temperature for 1 hour. Skin grafts were fixed in 4% v/v PFA for 24 hours and embedded in OCT. Sections were stained for CD8α (eBioscience; clone# 53–6.7) or Ly6G/C (eBioscience; RB6–8C5) and counterstained with DAPI. Images were recorded using an Olympus Provis fluorescent microscope (Ly6G/C) or an Olympus Fluoview 1000 confocal microscope (CD8).

2.8. Skin DC migration assay and phenotypic analysis

One percent v/v FITC (Sigma Aldrich; cat # F3651) in 1:1 acetone: dibutyl phthalate was applied to the dorsal surface of the ear pinna and 24 hours later, cells were isolated from the superficial and deep cervical LN. They were stained with mAbs against CD11c (clone #N418), I-A^b (AF6–120.1), CCR7 (4B12), CD86 (GL-1) and B7-H1 (10F 9G2) (all BioLegend), then fixed with 2% v/v PFA. Flow cytometry and data analysis were performed as described above (2.5).

2.9. Statistical analyses

Results are expressed as means ± 1SD. Significances of differences between groups were determined via either Log-rank test (survival curves), Student's 't'-test, or one-way ANOVA Tukey's multiple comparisons test (GraphPad Prism) as indicated, with $p < 0.05$ considered significant.

3. RESULTS

3.1. HY-mismatched skin grafts from TORC2$^{DC-/-}$ donors exhibit more severe rejection

We first grafted trunk skin from either WT control B6 males (Ctrl M) or TORC2$^{DC-/-}$ B6 males (TORC2$^{DC-/-}$ M) onto WT B6 males or females (Ctrl F). Ctrl M→ Ctrl M grafts were maintained intact > 60 days, after which the experiment was terminated, while TORC2$^{DC-/-}$ M→ Ctrl F grafts failed significantly more rapidly than Ctrl M→ Ctrl F grafts (median graft survival times [MST]:22.5 and 17 days, respectively; Figure 1A). Grafts from TORC2$^{DC-/-}$ M donors were also significantly smaller post-transplant compared with those from Ctrl M donors (Figure 1B). At POD 14 there was evidence of necrosis in the TORC2$^{DC-/-}$ grafts (Figure 1C). Before transplant, the epidermis, dermis and hair follicles of TORC2$^{DC-/-}$ donor skin did not differ histologically from normal Ctrl skin (Figure 1D). Banff scoring at POD 14, however, confirmed more severe rejection in TORC2$^{DC-/-}$ M→

Ctrl F compared with Ctrl M→ Ctrl F grafts (Figure 1E, F). The histological appearance of grafts at POD 7 indicating earlier pathological changes in TORC2$^{DC-/-}$ M → Ctrl F grafts is shown in Figure S1.

3.2. HY-mismatched skin grafts from TORC2$^{DC-/-}$ donors exhibit enhanced CD8$^+$ T cell infiltrates

To characterize the role of host immune cells in graft failure, we first used immunohistochemistry (IHC) to identify CD3$^+$ cells (Figure 2A, B) and immunofluorescence staining to identify CD8$^+$ cells (Figure 2C, D) in grafts at POD 7. More marked CD8$^+$ cell infiltration was observed in the TORC2$^{DC-/-}$ M→ Ctrl F compared with Ctrl M→ Ctrl F grafts, consistent with their accelerated rejection. By POD 14, absolute numbers of T cells in the TORC2$^{DC-/-}$ grafts were lower than those in Ctrl grafts, coinciding with more extensive tissue injury/collagen degradation in the former (Figure S1).

To further characterize T cell infiltrates within the grafts, we quantified total CD4$^+$ T effector cells (Teff; CD4$^+$Foxp3$^-$), CD8$^+$ T cells and Teff:regulatory T cell (Treg; CD4$^+$ Forkhead box p3$^+$ [Foxp3$^+$]) ratios (Figure 3A). Both Ctrl M→ Ctrl F grafts and TORC2$^{DC-/-}$ M→ Ctrl F grafts showed significant increases in CD4$^+$ Teff and CD8$^+$ cells, as well as augmented ratios of Teff :Treg; however, TORC2$^{DC-/-}$ grafts showed enriched CD8$^+$ T cell infiltrates compared to Ctrl grafts. There was also a significant increase in the number of CD8$^+$PD-1$^+$ T cells in the TORC2$^{DC-/-}$ compared to Ctrl grafts (Figure 3B, C), although no significant difference in the intensity of PD-1 expression.

3.3. Skin grafts from TORC2$^{DC-/-}$ donors elicit enhanced CD8$^+$ T effector cell responses in regional LN and augmented IFNγ and IL-2 production in response to donor Ag stimulation

To investigate host T cell function in graft recipients, T cells were isolated from draining axillary LN on POD 7 for quantitative and functional analysis (Figure 4). While there were significantly more CD4$^+$ Teff and an increased ratio of Teff:Treg in the Ctrl M→ Ctrl F and TORC2$^{DC-/-}$ M→ Ctrl F graft recipients than in the Ctrl M→ Ctrl M group, there was no significant difference between the former two groups. However, as observed within the graft itself, CD8$^+$ T cell numbers were increased significantly within draining LN of the TORC2$^{DC-/-}$ M→ Ctrl F recipients compared with the M→ Ctrl F recipients (Figure 4A; center panel). Cytokine production (IFNγ and IL-2) by LN T cells from recipients of TORC2$^{DC-/-}$ grafts in response to donor male Ag stimulation was greater than that by T cells from recipients of normal Ctrl grafts. There were, however, no differences in the very low levels of IL-4 production between groups (Figure 4B).

3.4. MHC-mismatched skin grafts from TORC2$^{DC-/-}$ donors also elicit enhanced CD8$^+$ T cell responses in regional LN

We next determined whether mTORC2 deficiency in donor DC might affect rejection in a full MHC-mismatch model, in which the donor-reactive CD8$^+$ T cell precursor frequency is higher than with a non-MHC minor Ag mismatch. We grafted full-thickness trunk skin from either WT BALB/c, WT control B6 (Ctrl B6) or TORC2$^{DC-/-}$ B6 mice onto WT BALB/c recipients. BALB/c→ BALB/c grafts were maintained intact for > 30 days, while

TORC2$^{DC-/-}$ B6→ BALB/c grafts and Ctrl B6→ BALB/c grafts were rejected acutely with similar graft survival times (MST: 8 and 9 days, respectively) (Figure 5A, B). Banff rejection scores at POD 5 were enhanced significantly in the TORC2$^{DC-/-}$ donor group (Figure 5C, D), although absolute numbers of graft-infiltrating CD3$^+$ and CD8$^+$ T cells were not increased (Figure S2).

T cells isolated from draining axillary LN on POD 5 exhibited significant increases in CD4$^+$ Teff and CD8$^+$ T cells in both the Ctrl B6 and TORC2$^{DC-/-}$ B6 donor groups compared to the syngeneic BALB/c donor control group, while the TORC2$^{DC-/-}$ donor group had significantly more CD8$^+$ T cells than the Ctrl B6 donor group (Figure 6A; left and **center panels**). There were no differences in the ratio of Teff:Treg between groups (Figure 6A; **right panel**). We also observed that while there were minimal CD8$^+$PD-1$^+$ cells in the BALB/c and Ctrl B6 donor groups, these cells were increased significantly in the TORC2$^{DC-/-}$ B6 donor group. No difference in intensity of PD-1 expression was observed between the groups (Figure 6B, C).

While there were no significant differences in the incidences of proliferating (CFSE^{lo}) CD4$^+$ Teff (Figure 7A; **top panel**) or the division index of Teff between the groups (Figure 7A; **bottom panel**), there were significant increases in proliferating CD8$^+$ T cells in both the Ctrl B6 and TORC2$^{DC-/-}$ B6 donor groups compared to the syngeneic BALB/c donor group (Figure 7B; **top panel**). Moreover, the CD8$^+$ T cell division index was augmented significantly in the TORC2$^{DC-/-}$ B6 donor group compared with both the BALB/c→ BALB/c and Ctrl B6→ BALB/c groups (Figure 7B, **bottom panel**). Furthermore, while both the Ctrl B6 and TORC2$^{DC-/-}$ B6 donor groups showed significantly elevated IFNγ, IL-2 and GrB production compared to the syngeneic BALB/c donor group in response to donor B6 Ag stimulation, T cells from the TORC2$^{DC-/-}$ donor group produced significantly more IFNγ and GrB compared to the Ctrl B6 donor group (Figure 7D).

3.5. TORC2$^{DC-/-}$ mice exhibit enhanced cutaneous DTH responses

Next,we sought to confirm the pro-inflammatory function of TORC2$^{-/-}$ DC in donor skin. Utilizing a cell-mediated DTH model in which the skin was sensitized with DNFB, then challenged 5 days later with DNFB, TORC2$^{DC-/-}$ mice exhibited significant increases in responses compared with WT Ctrl animals (Figure 8A). These enhanced responses were accompanied by increases in epidermal thickness (Figure 8B) and significant increases in CD8$^+$ T cell infiltration (Figure 8C, D). Moreover, significant increases in skin-infiltrating Ly6G/C$^+$ cells (Figure 8E, F) were also observed in TORC2$^{DC-/-}$ mice.

3.6. TORC2$^{DC-/-}$ mice display a more pro-stimulatory DC phenotype than WT Ctrl mice

To ascertain whether the augmented cutaneous cell-mediated inflammatory responses observed in TORC2$^{DC-/-}$ mice could be ascribed to altered DC phenotype and/or DC migratory capacity, we painted ear pinnae of TORC2$^{DC-/-}$ or WT Ctrl mice with FITC. After 24 hours, cells in the draining superficial and deep cervical LN were isolated and migratory DC identified as FITC$^+$. There were no significant differences between WT Ctrl and TORC2$^{DC-/-}$ mice in terms of total number of CD11c$^+$IA$^{b\ hi}$ DC (Figure 9A), FITC $^+$CD11c$^+$I-A$^{b\ hi}$ DC (Figure 9B), FITC expression by DC (Figure 9C) or CCR7 expression

on FITC$^+$ DC (Figure 9D). These data indicate that mTORC2$^{-/-}$ DC did not differ in their migratory capacity compared with Ctrl DC. On the other hand, while co-stimulatory CD86 expression did not differ on migrating FITC$^+$ DC between WT Ctrl and TORC2$^{DC-/-}$ mice (Figure 9E), co-inhibitory B7-H1 expression was reduced significantly on the migrating mTORC2$^{-/-}$ DC compared to WT Ctrl DC (Figure 9F), suggesting enhanced T cell stimulatory potential of the LN-homing mTORC2-deficient skin DC.

3.7. Skin graft rejection is not affected in TORC2$^{DC-/-}$ recipients

Having observed that mTORC2 deficiency in donor DC led to accelerated minor H Ag-mismatched skin graft rejection, we also investigated whether, conversely, mTORC2 deficiency only in recipient DC might also affect graft rejection. We grafted trunk skin from either B6 WT Ctrl mice (OVA$^-$) or OVAtg mice (OVA$^+$) onto syngeneic B6 WT Ctrl or TORC2$^{DC-/-}$ mice. While all OVA$^-$ → Ctrl grafts remained intact after 25 days, the MST for OVA$^+$ → TORC2$^{DC-/-}$ and OVA$^+$ → Ctrl grafts were 16.5 and 18.5 days respectively, and did not differ significantly (Figure S3A). The OVA$^+$ grafts were reduced slightly but significantly in size 21 and 23 days post-transplant in TORC2$^{DC-/-}$ compared to Ctrl recipients (Figure S3B). Gross morphology of the grafts on POD 14 showed more extensive necrosis of both the OVA$^+$ → Ctrl and OVA$^+$ → TORC2$^{DC-/-}$ grafts compared to those from OVA$^-$ donors (Figure S3C). Histological examination and Banff criteria scores confirmed similar levels of rejection in the OVA$^+$ → TORC2$^{DC-/-}$ and OVA$^+$ → Ctrl grafts at POD 14 (Figure S3D, E), and there were no significant differences in CD3$^+$ and CD8$^+$ T cell infiltration (Figures S4 **and** S5). There were also no significant differences in the numbers of CD4$^+$ Teff or CD8$^+$ T cells or in the Teff:Treg ratio in regional LN between the OVA$^+$→TORC2$^{DC-/-}$ and OVA$^+$→Ctrl groups and cytokine production was not affected (Figure S6). Thus, in contrast to transplants from TORC2$^{DC-/-}$ donors in WT recipients, grafts from donors with intact DC to TORC2$^{DC-/-}$ recipients did not exhibit augmented T cell responses or increased tissue injury.

4. DISCUSSION

We have reported previously[23] that ex vivo-generated, conventional BM-derived myeloid DC lacking functional mTORC2 display an enhanced pro-inflammatory phenotype and can augment allogeneic Th1/Th17 polarization and proliferation in vitro, as well as Ag-specific Th1/Th17 responses in vivo. We now show, using a non MHC-mismatched (M→F) transplant model in which rejection occurs in response to male HY Ag[32], that TORC2$^{DC-/-}$ skin grafts undergo accelerated rejection, accompanied by enhanced CD8$^+$ T cell responses. While it has been reported that conditional disruption of mTORC1 in DC dysregulates epidermal Langerhans cell (LC) homeostasis[33] and that, based on inactivation of mTOR complexes specifically in the epidermis, both mTORC1 and mTORC2 in keratinocytes are integral components of skin morphogenesis[34], conditional deletion of mTORC2 in DC does not impact skin morphogenesis. Moreover, in the present study, histological comparison of naïve trunk skin between TORC2$^{DC-/-}$ and WT B6 male skin did not reveal any morphological differences. Thus, inherent anatomic or skin-resident DC homeostatic abnormalities are unlikely to account for the accelerated failure/rejection of TORC2$^{DC-/-}$ grafts that we observed.

Donor DC are required for direct priming of immune responses to Ags expressed by MHC-mismatched grafts. With MHC-matched, minor H Ag-mismatched grafts (such as donor male skin grafts in syngeneic female recipients), the intensity of the T cell response to directly-presented Ags is reduced, while the indirect pathway of Ag recognition is also thought to be important[35]. However, conditional depletion of epidermal LC or conventional dermal DC in male skin grafts prolongs graft survival but does not prevent their rejection in female recipients[35] and delayed rejection is correlated with delayed expansion of HY Ag-specific $CD8^+$ T cells. Therefore, the ability of interstitial donor $mTORC2^{-/-}$ DC in this study to elicit enriched $CD8^+$ T cell responses not only highlights the importance of $CD8^+$ T cells in graft rejection, but also mirrors our previous finding that intratumoral injection of syngeneic BM-derived $mTORC2^{-/-}$ DC delays B16 melanoma growth in a $CD8^+$ T cell-dependent manner[36]. Moreover, the increased incidence of $CD8^+PD\text{-}1^+$ T cells elicited by interstitial donor $mTORC2^{-/-}$ DC suggests these T cells are also more activated, as PD-1 expression has been used to identify tumor-reactive $CD8^+$ tumor-infiltrating T cells[37, 38]. Although overexpression of PD-1 has been associated with T cell exhaustion[39], we did not observe any significant differences in the intensity of PD-1 expression by graft-infiltrating $CD8^+$ $PD\text{-}1^+$ T cells.

As we observed within the minor H Ag-mismatched grafts, elevated numbers of $CD8^+$ T cells were also found in regional LN of $TORC2^{DC-/-}$ skin recipients. Moreover, $TORC2^{DC-/-}$ graft recipient T cells produced elevated levels of pro-inflammatory IFNγ and IL-2 in response to donor Ag stimulation. IFNγ is well-known to skew $CD4^+$ T cell responses to a Th1 phenotype[40] and has also been implicated in direct control of $CD8^+$ T cell expansion[41].

In addition to enhanced T cell infiltration, we also observed greater collagen degradation in the minor H Ag-mismatched $TORC2^{DC-/-}$ grafts. Collagen degradation is found in rejecting bilayered skin constructs grafted onto patients with chronic wound-healing defects[42] and collagen type I formation is a positive indicator of graft survival in facial plastic and reconstructive surgery[43]. Thus, pronounced collagen degradation in the $TORC2^{DC-/-}$ skin grafts provides additional evidence of their enhanced rejection compared to WT grafts.

We also investigated whether DC-specific mTORC2 deficiency in donor grafts would accelerate rejection in a full-MHC mismatch model, in which the donor Ag-specific precursor T cell population is larger than that in a non-MHC mismatch, minor mismatch model. Although there was a trend for $TORC2^{DC-/-}$ B6 → BALB/c grafts to fail more rapidly than Ctrl B6 → BALB/c grafts, this was not statistically significant. However, draining LN of the $TORC2^{DC-/-}$ graft recipients contained more activated $CD8^+$ T cells, based on their expression of PD-1. Moreover, when stimulated with donor Ag, $CD8^+$ T cells from $TORC2^{DC-/-}$ graft recipients had a significantly higher division index, indicative of multiple divisions per cell. In addition, LN T cells from $TORC2^{DC-/-}$ graft recipients produced more IFNγ and GrB than Ctrl graft recipient T cells. As it has been demonstrated that $CD8^+$ T cells are critical for the production of GrB in rejecting skin grafts[44], this provides further evidence of the augmented ability of $mTORC2^{-/-}$ DC to stimulate $CD8^+$ T cells in the context of skin transplantation.

Defects in wound healing can cause graft displacement and loss of function[45], while treatment of transplant recipients with the mTORC1 inhibitor rapamycin impairs wound healing via its lymphopenic properties[46]. However, we do not believe that impaired wound healing contributed to the accelerated rejection of TORC2$^{DC-/-}$ grafts as this effect has not been ascribed to mTORC2 inhibition. Additionally, since DC and T cells positively regulate wound healing[47] and since mTORC2$^{-/-}$ DC augment graft T cell infiltration, impaired wound healing is considered unlikely.

The enhanced cutaneous DTH responses we observed in TORC2$^{DC-/-}$ compared to Ctrl mice were characterized by increased CD8^{+} T cell and Ly6C/G^{+} myeloid cell infiltration, confirming that the absence of functional mTORC2 in skin-resident DC induced augmented cutaneous cell-mediated immunity. The type of responses that we examined (T cell-mediated contact hypersensitivity) are dependent on epidermal immunomodulatory LC that express CD11c[48], capture the sensitizing hapten and migrate to regional LN for direct presentation to CD8^{+} T cells (the predominant effectors of contact hypersensitivity[49–51]) and also on dermal DC[52] that can also play essential roles in inducing immunity[53, 54]. Since LC have also been shown to dampen murine contact hypersensitivity responses by tolerizing CD8^{+} T cells[55, 56], the augmented responses seen in TORC2$^{DC-/-}$ skin may be a consequence of reduction in their immunoregulatory function.

Previous studies have implicated mTORC2 in regulation of cell migration. Thus, breast cancer cells lacking mTORC2 exhibit reduced migratory function[57]. Whether mTORC2 affects skin DC migration following hapten sensitization has not previously been examined. We therefore considered whether the enhanced cutaneous cell-mediated immune reactions that we observed in TORC2$^{DC-/-}$ mice might reflect altered migration of skin-resident TORC2$^{DC-/-}$ to secondary lymphoid tissue. However, we saw no significant differences in skin DC migration to regional LN between Ctrl and TORC2$^{DC-/-}$ mice, or in acquisition/expression of the sensitizing agent by migrating, hapten-expressing (FITC^{+}) DC between Ctrl DC and TORC2$^{DC-/-}$ DC. There was also no significant difference in the expression by these DC of CCR7 that guides their migration to cognate ligands in secondary lymphoid tissue[58]. Taken together, these data suggest that the accelerated rejection of minor H Ag-mismatched TORC2$^{DC-/-}$ skin grafts and the enhanced cutaneous DTH responses in TORC2$^{DC-/-}$ mice are not due to alterations in DC migration to regional lymphoid tissue. Interestingly, however, migratory mTORC2-deficient DC displayed decreased cell surface B7-H1 expression relative to unmodified costimulatory CD86 expression, indicative of a more T cell stimulatory phenotype and providing further evidence that skin-resident DC that specifically lack mTORC2 are more immunostimulatory than Ctrl skin-resident DC.

In the present study, we also examined, conversely, the fate of WT skin grafts in TORC2$^{DC-/-}$ recipients. Donor-derived DC have long been regarded (via the direct pathway of allorecognition) as instigators of acute, MHC-mismatched allograft rejection, but are thought to be eliminated soon after transplant, while host DC have been implicated (via the indirect pathway) in development/maintenance of chronic rejection. Recent evidence[59] acquired using the tg OVA Ag skin transplant model suggests however that, by acquiring intact donor MHC class I Ag (semi-direct allorecognition) host DC may play an essential role in the instigation/regulation of acute rejection. Utilizing this OVAtg skin transplant

model in which OVA functions as a minor H Ag[60] to investigate whether mTORC2 deficiency in host DC that indirectly/semi-directly present donor Ag affects skin graft outcome, we did not observe any significant difference in graft rejection. OVA may not be captured efficiently by recipient APC that repopulate the graft[60] with the result that absence of mTORC2 in host DC does not significantly affect graft survival. Pronounced $CD8^+$ T cell infiltrates were observed in both WT Ctrl and $TORC2^{DC-/-}$ recipients of these minor H Ag-mismatched grafts at POD 7. When considered together with the data showing no differences in numbers of $CD4^+$ Teff, $CD8^+$ T cells or $CD4^+$Treg at POD 7 within regional LN, or differences in cytokine production following host T cell challenge with OVA^+ DC, it appears that selective mTORC2 deficiency in recipient DC does not affect T cell-mediated graft rejection in this model.

Our findings describe for the first time, a role for mTORC2 in graft-resident DC in the regulation of transplant outcome. In a model of minor H Ag (HY)-mismatched skin graft rejection, mTORC2 deficiency in donor DC elicited enhanced effector $CD8^+$ T cell responses, consistent with accelerated rejection. The ability of tissue-resident DC deficient in mTORC2 function to augment anti-donor $CD8^+$ T cell responses should be considered in interpreting the influence of mTOR inhibitors on immune reactivity, and in the development of new generation dual mTORC1 and 2 inhibitors[14] and selective mTORC2 inhibitors[16, 17].

Supplementary Material

Refer to Web version on PubMed Central for supplementary material.

ACKNOWLEDGMENTS

This work was supported by NIH grants R01 AI67541 and R01 AI1188777 (to AWT) and by research funds provided by the Starzl Transplantation Institute. ARW was the recipient of an institutional T32 training grant predoctoral fellowship (T32 AI74490 to AWT). We thank Dr. Dalia Raich-Regue for critical review of the manuscript and the University of Pittsburgh Center for Biological Imaging for technological support.

Abbreviations:

Ag	antigen
Ctrl	control
DC(s)	dendritic cell(s)
LN(s)	lymph node(s)
mTOR(C)	mechanistic target of rapamycin (complex)
MFI	mean fluorescence intensity
OVA	ovalbumin
POD	post-operative day
tg	transgenic

WT wild-type

REFERENCES

1. Wullschleger S, Loewith R, Hall MN. TOR signaling in growth and metabolism. Cell 2006;124(3): 471–484. [PubMed: 16469695]
2. Yang Q, Guan KL. Expanding mTOR signaling. Cell research 2007;17(8):666–681. [PubMed: 17680028]
3. Fantus D, Rogers NM, Grahammer F, Huber TB, Thomson AW. Roles of mTOR complexes in the kidney: implications for renal disease and transplantation. Nature reviews Nephrology 2016;12(10): 587–609. [PubMed: 27477490]
4. Thomson AW, Turnquist HR, Raimondi G. Immunoregulatory functions of mTOR inhibition. Nature reviews Immunology 2009;9(5):324–337.
5. Powell JD, Delgoffe GM. The mammalian target of rapamycin: linking T cell differentiation, function, and metabolism. Immunity 2010;33(3):301–311. [PubMed: 20870173]
6. Oh MH, Collins SL, Sun IH, Tam AJ, Patel CH, Arwood ML et al. mTORC2 Signaling Selectively Regulates the Generation and Function of Tissue-Resident Peritoneal Macrophages. Cell reports 2017;20(10):2439–2454. [PubMed: 28877476]
7. Fantus D, Thomson AW. Evolving perspectives of mTOR complexes in immunity and transplantation. American journal of transplantation : official journal of the American Society of Transplantation and the American Society of Transplant Surgeons 2015;15(4):891–902.
8. Laplante M, Sabatini DM. mTOR signaling in growth control and disease. Cell 2012;149(2):274–293. [PubMed: 22500797]
9. Sarbassov DD, Ali SM, Kim DH, Guertin DA, Latek RR, Erdjument-Bromage H et al. Rictor, a novel binding partner of mTOR, defines a rapamycin-insensitive and raptor-independent pathway that regulates the cytoskeleton. Current biology : CB 2004;14(14):1296–1302. [PubMed: 15268862]
10. Sarbassov DD, Ali SM, Sengupta S, Sheen JH, Hsu PP, Bagley AF et al. Prolonged rapamycin treatment inhibits mTORC2 assembly and Akt/PKB. Molecular cell 2006;22(2):159–168. [PubMed: 16603397]
11. Lamming DW, Ye L, Katajisto P, Goncalves MD, Saitoh M, Stevens DM et al. Rapamycin-induced insulin resistance is mediated by mTORC2 loss and uncoupled from longevity. Science 2012;335(6076):1638–1643. [PubMed: 22461615]
12. Rosborough BR, Raich-Regue D, Matta BM, Lee K, Gan B, DePinho RA et al. Murine dendritic cell rapamycin-resistant and rictor-independent mTOR controls IL-10, B7-H1, and regulatory T-cell induction. Blood 2013;121(18):3619–3630. [PubMed: 23444404]
13. Schreiber KH, Ortiz D, Academia EC, Anies AC, Liao CY, Kennedy BK. Rapamycin-mediated mTORC2 inhibition is determined by the relative expression of FK506-binding proteins. Aging cell 2015;14(2):265–273. [PubMed: 25652038]
14. Rosborough BR, Raich-Regue D, Liu Q, Venkataramanan R, Turnquist HR, Thomson AW. Adenosine triphosphate-competitive mTOR inhibitors: a new class of immunosuppressive agents that inhibit allograft rejection. American journal of transplantation : official journal of the American Society of Transplantation and the American Society of Transplant Surgeons 2014;14(9):2173–2180.
15. Fantus D, Dai H, Ono Y, Watson A, Yokota S, Mohib K et al. Influence of the Novel ATP-Competitive Dual mTORC1/2 Inhibitor AZD2014 on Immune Cell Populations and Heart Allograft Rejection. Transplantation 2017;101(12):2830–2840. [PubMed: 28885497]
16. Schmidt KM, Hellerbrand C, Ruemmele P, Michalski CW, Kong B, Kroemer A et al. Inhibition of mTORC2 component RICTOR impairs tumor growth in pancreatic cancer models. Oncotarget 2017;8(15):24491–24505. [PubMed: 28445935]
17. Werfel TA, Wang S, Jackson MA, Kavanaugh TE, Joly MM, Lee LH et al. Selective mTORC2 Inhibitor Therapeutically Blocks Breast Cancer Cell Growth and Survival. Cancer research 2018;78(7):1845–1858. [PubMed: 29358172]

18. Delgoffe GM, Pollizzi KN, Waickman AT, Heikamp E, Meyers DJ, Horton MR et al. The kinase mTOR regulates the differentiation of helper T cells through the selective activation of signaling by mTORC1 and mTORC2. Nature immunology 2011;12(4):295–303. [PubMed: 21358638]
19. Pollizzi KN, Patel CH, Sun IH, Oh MH, Waickman AT, Wen J et al. mTORC1 and mTORC2 selectively regulate CD8(+) T cell differentiation. The Journal of clinical investigation 2015;125(5):2090–2108. [PubMed: 25893604]
20. Zhang L, Tschumi BO, Lopez-Mejia IC, Oberle SG, Meyer M, Samson G et al. Mammalian Target of Rapamycin Complex 2 Controls CD8 T Cell Memory Differentiation in a Foxo1-Dependent Manner. Cell reports 2016;14(5):1206–1217. [PubMed: 26804903]
21. Jiang H, Westerterp M, Wang C, Zhu Y, Ai D. Macrophage mTORC1 disruption reduces inflammation and insulin resistance in obese mice. Diabetologia 2014;57(11):2393–2404. [PubMed: 25120095]
22. Ohtani M, Hoshii T, Fujii H, Koyasu S, Hirao A, Matsuda S. Cutting edge: mTORC1 in intestinal CD11c+ CD11b+ dendritic cells regulates intestinal homeostasis by promoting IL-10 production. Journal of immunology 2012;188(10):4736–4740.
23. Raich-Regue D, Rosborough BR, Watson AR, McGeachy MJ, Turnquist HR, Thomson AW. mTORC2 Deficiency in Myeloid Dendritic Cells Enhances Their Allogeneic Th1 and Th17 Stimulatory Ability after TLR4 Ligation In Vitro and In Vivo. Journal of immunology 2015.
24. Billingham RE, Brent L, Medawar PB. Actively acquired tolerance of foreign cells. Nature 1953;172(4379):603–606. [PubMed: 13099277]
25. Atif SM, Nelsen MK, Gibbings SL, Desch AN, Kedl RM, Gill RG et al. Cutting Edge: Roles for Batf3-Dependent APCs in the Rejection of Minor Histocompatibility Antigen-Mismatched Grafts. Journal of immunology 2015;195(1):46–50.
26. Fischer S, Lian CG, Kueckelhaus M, Strom TB, Edelman ER, Clark RA et al. Acute rejection in vascularized composite allotransplantation. Current opinion in organ transplantation 2014;19(6): 531–544. [PubMed: 25333831]
27. Kanitakis J, Petruzzo P, Gazarian A, Karayannopoulou G, Buron F, Dubois V et al. Capillary Thrombosis in the Skin: A Pathologic Hallmark of Severe/Chronic Rejection of Human Vascularized Composite Tissue Allografts? Transplantation 2016;100(4):954–957. [PubMed: 27003099]
28. Maraskovsky E, Brasel K, Teepe M, Roux ER, Lyman SD, Shortman K et al. Dramatic increase in the numbers of functionally mature dendritic cells in Flt3 ligand-treated mice: multiple dendritic cell subpopulations identified. The Journal of experimental medicine 1996;184(5):1953–1962. [PubMed: 8920882]
29. Diaz-Perez JA, Killeen ME, Yang Y, Carey CD, Falo LD, Jr., Mathers AR. Extracellular ATP and IL-23 form a local inflammatory circuit leading to the development of a neutrophil-dependent psoriasiform dermatitis. The Journal of investigative dermatology 2018;In press.
30. Kaplan DH, Jenison MC, Saeland S, Shlomchik WD, Shlomchik MJ. Epidermal langerhans cell-deficient mice develop enhanced contact hypersensitivity. Immunity 2005;23(6):611–620. [PubMed: 16356859]
31. Mathers AR, Carey CD, Killeen ME, Diaz-Perez JA, Salvatore SR, Schopfer FJ et al. Electrophilic nitro-fatty acids suppress allergic contact dermatitis in mice. Allergy 2017;72(4):656–664. [PubMed: 27718238]
32. Eichwald EJ, Silmser CR. Skin. Transplantation bulletin 1955;2:148–149. [PubMed: 12334405]
33. Kellersch B, Brocker T. Langerhans cell homeostasis in mice is dependent on mTORC1 but not mTORC2 function. Blood 2013;121(2):298–307. [PubMed: 23212520]
34. Ding X, Bloch W, Iden S, Ruegg MA, Hall MN, Leptin M et al. mTORC1 and mTORC2 regulate skin morphogenesis and epidermal barrier formation. Nature communications 2016;7:13226.
35. Fernandes E, Goold HD, Kissenpfennig A, Malissen B, Dyson J, Bennett CL. The role of direct presentation by donor dendritic cells in rejection of minor histocompatibility antigen-mismatched skin and hematopoietic cell grafts. Transplantation 2011;91(2):154–160. [PubMed: 21085063]
36. Raich-Regue D, Fabian KP, Watson AR, Fecek RJ, Storkus WJ, Thomson AW. Intratumoral delivery of mTORC2-deficient dendritic cells inhibits B16 melanoma growth by promoting CD8(+) effector T cell responses. Oncoimmunology 2016;5(6):e1146841. [PubMed: 27471613]

37. Inozume T, Hanada K, Wang QJ, Ahmadzadeh M, Wunderlich JR, Rosenberg SA et al. Selection of CD8+PD-1+ lymphocytes in fresh human melanomas enriches for tumor-reactive T cells. Journal of immunotherapy 2010;33(9):956–964. [PubMed: 20948441]
38. Gros A, Robbins PF, Yao X, Li YF, Turcotte S, Tran E et al. PD-1 identifies the patient-specific CD8(+) tumor-reactive repertoire infiltrating human tumors. The Journal of clinical investigation 2014;124(5):2246–2259. [PubMed: 24667641]
39. Wherry EJ. T cell exhaustion. Nature immunology 2011;12(6):492–499. [PubMed: 21739672]
40. Wakil AE, Wang ZE, Ryan JC, Fowell DJ, Locksley RM. Interferon gamma derived from CD4(+) T cells is sufficient to mediate T helper cell type 1 development. The Journal of experimental medicine 1998;188(9):1651–1656. [PubMed: 9802977]
41. Tewari K, Nakayama Y, Suresh M. Role of direct effects of IFN-gamma on T cells in the regulation of CD8 T cell homeostasis. Journal of immunology 2007;179(4):2115–2125.
42. Badiavas EV, Paquette D, Carson P, Falanga V. Human chronic wounds treated with bioengineered skin: histologic evidence of host-graft interactions. Journal of the American Academy of Dermatology 2002;46(4):524–530. [PubMed: 11907501]
43. Reksodiputro M, Widodo D, Bashiruddin J, Siregar N, Malik S. PRFM enhance wound healing process in skin graft. Facial plastic surgery : FPS 2014;30(6):670–675. [PubMed: 25536135]
44. Youssef AR, Otley C, Mathieson PW, Smith RM. Role of CD4+ and CD8+ T cells in murine skin and heart allograft rejection across different antigenic desparities. Transplant immunology 2004;13(4):297–304. [PubMed: 15589743]
45. Mehrabi A, Fonouni H, Wente M, Sadeghi M, Eisenbach C, Encke J et al. Wound complications following kidney and liver transplantation. Clinical transplantation 2006;20 Suppl 17:97–110.
46. Schaffer M, Schier R, Napirei M, Michalski S, Traska T, Viebahn R. Sirolimus impairs wound healing. Langenbeck's archives of surgery 2007;392(3):297–303.
47. Vinish M, Cui W, Stafford E, Bae L, Hawkins H, Cox R et al. Dendritic cells modulate burn wound healing by enhancing early proliferation. Wound repair and regeneration : official publication of the Wound Healing Society [and] the European Tissue Repair Society 2016;24(1):6–13.
48. Merad M, Ginhoux F, Collin M. Origin, homeostasis and function of Langerhans cells and other langerin-expressing dendritic cells. Nature reviews Immunology 2008;8(12):935–947.
49. Bour H, Peyron E, Gaucherand M, Garrigue JL, Desvignes C, Kaiserlian D et al. Major histocompatibility complex class I-restricted CD8+ T cells and class II-restricted CD4+ T cells, respectively, mediate and regulate contact sensitivity to dinitrofluorobenzene. European journal of immunology 1995;25(11):3006–3010. [PubMed: 7489735]
50. Martin S, Lappin MB, Kohler J, Delattre V, Leicht C, Preckel T et al. Peptide immunization indicates that CD8+ T cells are the dominant effector cells in trinitrophenyl-specific contact hypersensitivity. The Journal of investigative dermatology 2000;115(2):260–266. [PubMed: 10951244]
51. Vocanson M, Hennino A, Cluzel-Tailhardat M, Saint-Mezard P, Benetiere J, Chavagnac C et al. CD8+ T cells are effector cells of contact dermatitis to common skin allergens in mice. The Journal of investigative dermatology 2006;126(4):815–820. [PubMed: 16456532]
52. Honda T, Nakajima S, Egawa G, Ogasawara K, Malissen B, Miyachi Y et al. Compensatory role of Langerhans cells and langerin-positive dermal dendritic cells in the sensitization phase of murine contact hypersensitivity. The Journal of allergy and clinical immunology 2010;125(5):1154–1156 e1152. [PubMed: 20226508]
53. Fukunaga A, Khaskhely NM, Sreevidya CS, Byrne SN, Ullrich SE. Dermal dendritic cells, and not Langerhans cells, play an essential role in inducing an immune response. Journal of immunology 2008;180(5):3057–3064.
54. Henri S, Poulin LF, Tamoutounour S, Ardouin L, Guilliams M, de Bovis B et al. CD207+ CD103+ dermal dendritic cells cross-present keratinocyte-derived antigens irrespective of the presence of Langerhans cells. The Journal of experimental medicine 2010;207(1):189–206. [PubMed: 20038600]
55. Igyarto BZ, Jenison MC, Dudda JC, Roers A, Muller W, Koni PA et al. Langerhans cells suppress contact hypersensitivity responses via cognate CD4 interaction and langerhans cell-derived IL-10. Journal of immunology 2009;183(8):5085–5093.

56. Gomez de Aguero M, Vocanson M, Hacini-Rachinel F, Taillardet M, Sparwasser T, Kissenpfennig A et al. Langerhans cells protect from allergic contact dermatitis in mice by tolerizing CD8(+) T cells and activating Foxp3(+) regulatory T cells. The Journal of clinical investigation 2012;122(5): 1700–1711. [PubMed: 22523067]

57. Li H, Lin J, Wang X, Yao G, Wang L, Zheng H et al. Targeting of mTORC2 prevents cell migration and promotes apoptosis in breast cancer. Breast cancer research and treatment 2012;134(3):1057–1066. [PubMed: 22476852]

58. Riol-Blanco L, Sanchez-Sanchez N, Torres A, Tejedor A, Narumiya S, Corbi AL et al. The chemokine receptor CCR7 activates in dendritic cells two signaling modules that independently regulate chemotaxis and migratory speed. Journal of immunology 2005;174(7):4070–4080.

59. Smyth LA, Lechler RI, Lombardi G. Continuous Acquisition of MHC:Peptide Complexes by Recipient Cells Contributes to the Generation of Anti-Graft CD8(+) T Cell Immunity. American journal of transplantation : official journal of the American Society of Transplantation and the American Society of Transplant Surgeons 2017;17(1):60–68.

60. Ehst BD, Ingulli E, Jenkins MK. Development of a novel transgenic mouse for the study of interactions between CD4 and CD8 T cells during graft rejection. American journal of transplantation : official journal of the American Society of Transplantation and the American Society of Transplant Surgeons 2003;3(11):1355–1362.

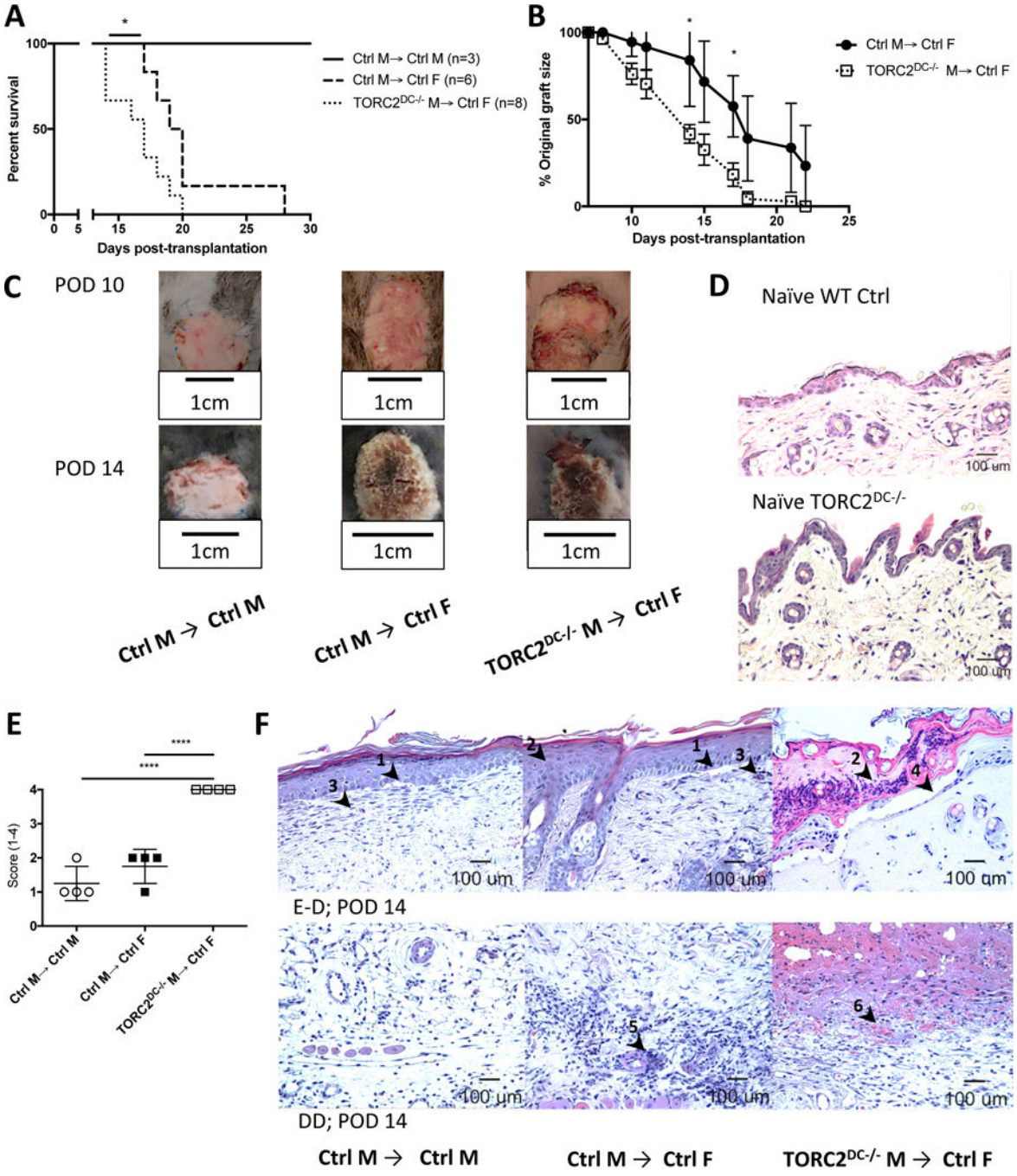

FIGURE 1.

HY-mismatched skin grafts from TORC2$^{DC-/-}$ donors exhibit shortened survival times and enhanced Banff ejection scores. Male (M) or female (F) wild-type B6 mice were transplanted with full-thickness skin grafts from either B6 WT control M (Ctrl M) or B6 TORC2$^{DC-/-}$ M donors. (A) Graft survival over time, *n=3–8* mice per group; Log-rank test, *, $p < 0.05$. (B) Skin graft size as a percentage of original graft size over time, *n=6–8* mice per group; Student's t-test, *, $p < 0.05$. (C) Representative gross morphology of skin grafts at post-operative day (POD) 10 and POD 14. (D) Representative H&E staining of normal

naïve (non-transplanted) WT Ctrl and TORC2$^{DC-/-}$ trunk skin. (E) Banff rejection scores of skin grafts at POD 14, *n=4;* one-way ANOVA Tukey's multiple comparisons test, ^{xxxx}, $p < 0.001$. (F) Representative H&E staining of skin grafts at POD 14 showing (above) the epidermal-dermal junction (E-D) and (below) the deep dermal layer (DD). Arrowheads indicate (1) vacuolar damage, (2) pathological diskeratosis, (3) lichenoid infiltrate/interface dermatitis, (4) pemphigoid acantholysis, (5) vasculitis and (6) thrombosis.

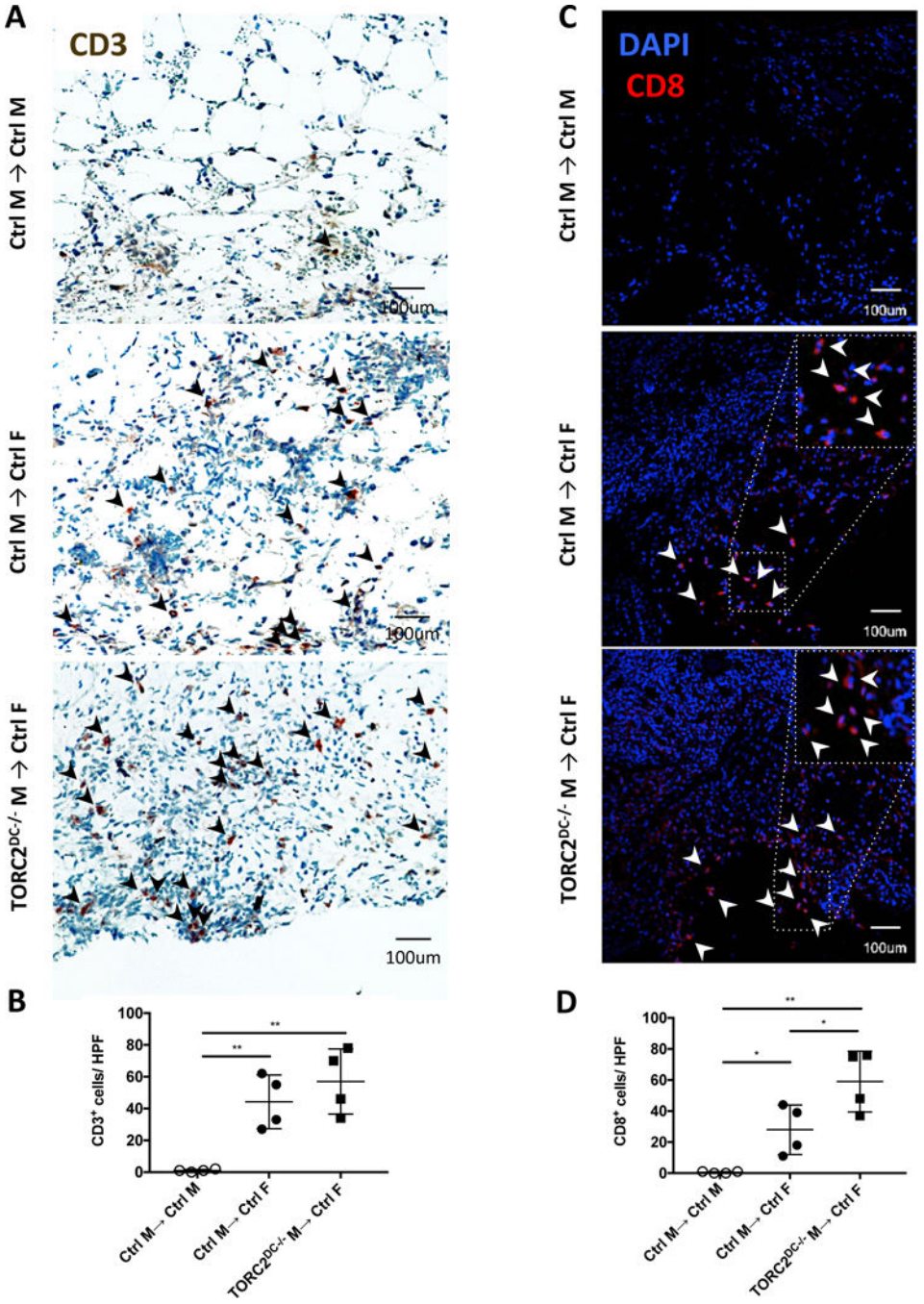

FIGURE 2.

HY-mismatched skin grafts from TORC2$^{DC-/-}$ donors elicit enhanced CD8^{+} T cell infiltration. Quantitative analysis of T cell infiltration in skin grafts from WT control (Ctrl) M and TORC2$^{DC-/-}$ M donors was performed on post-operative day (POD) 7. (A) Representative immunohistochemical staining for CD3^{+} cells (arrowheads); *n=4* mice per group. (B) Numbers of CD3^{+} cells per high power field (hpf) in skin grafts; *n=4* mice per group; one-way ANOVA Tukey's multiple comparisons test, ***, p<0.01.* (C) Representative staining for CD8^{+} cells (arrowheads); *n=4* mice per group. (D) Numbers of CD8^{+} cells per

hpf in skin grafts; *n=4* mice per group; one-way ANOVA Tukey's multiple comparisons test, *, $p < 0.05$; **, $p<0.01$.

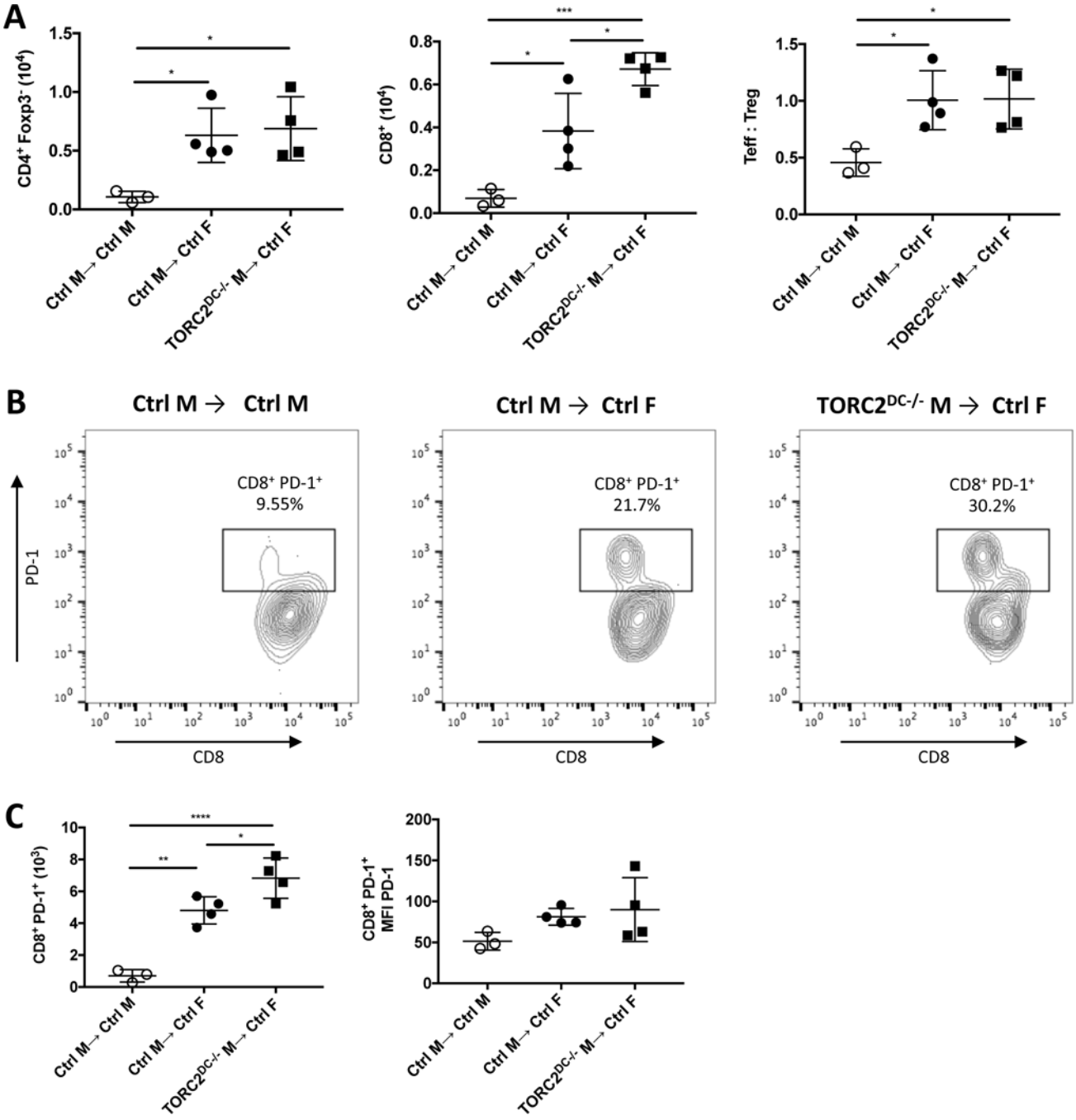

FIGURE 3.

HY-mismatched skin grafts from TORC2DC$^{-/-}$ male (M) donors exhibit enhanced CD8^{+}PD-1^{+} T cell infiltration compared with grafts from WT control (Ctrl) M donors. Cells were isolated from skin grafts on post-operative day (POD) 7 via collagenase digestion and analyzed following mAb staining by flow cytometry. T cells were gated on live (Zombie^{-}) CD45.2^{+}CD3^{+} cells. (A) Total numbers of CD4^{+}Foxp3^{-} T effector (Teff) cells, CD8^{+} cells and Teff:CD4^{+}Foxp3^{+} (Treg) cell ratios within the grafts. (B) Representative histograms of CD8^{+}PD-1^{+} T cells within the grafts. (C) Numbers of CD8^{+}PD-1^{+} T cells within the grafts

(left) and mean fluorescence intensity (MFI) of PD-1 on PD-1$^+$ cells (right). *n=4* mice per group; one-way ANOVA Tukey's multiple comparisons test, *, *p < 0.05; **, p<0.01*, ***, *p<0.001*, ****, *p<0.0001.*

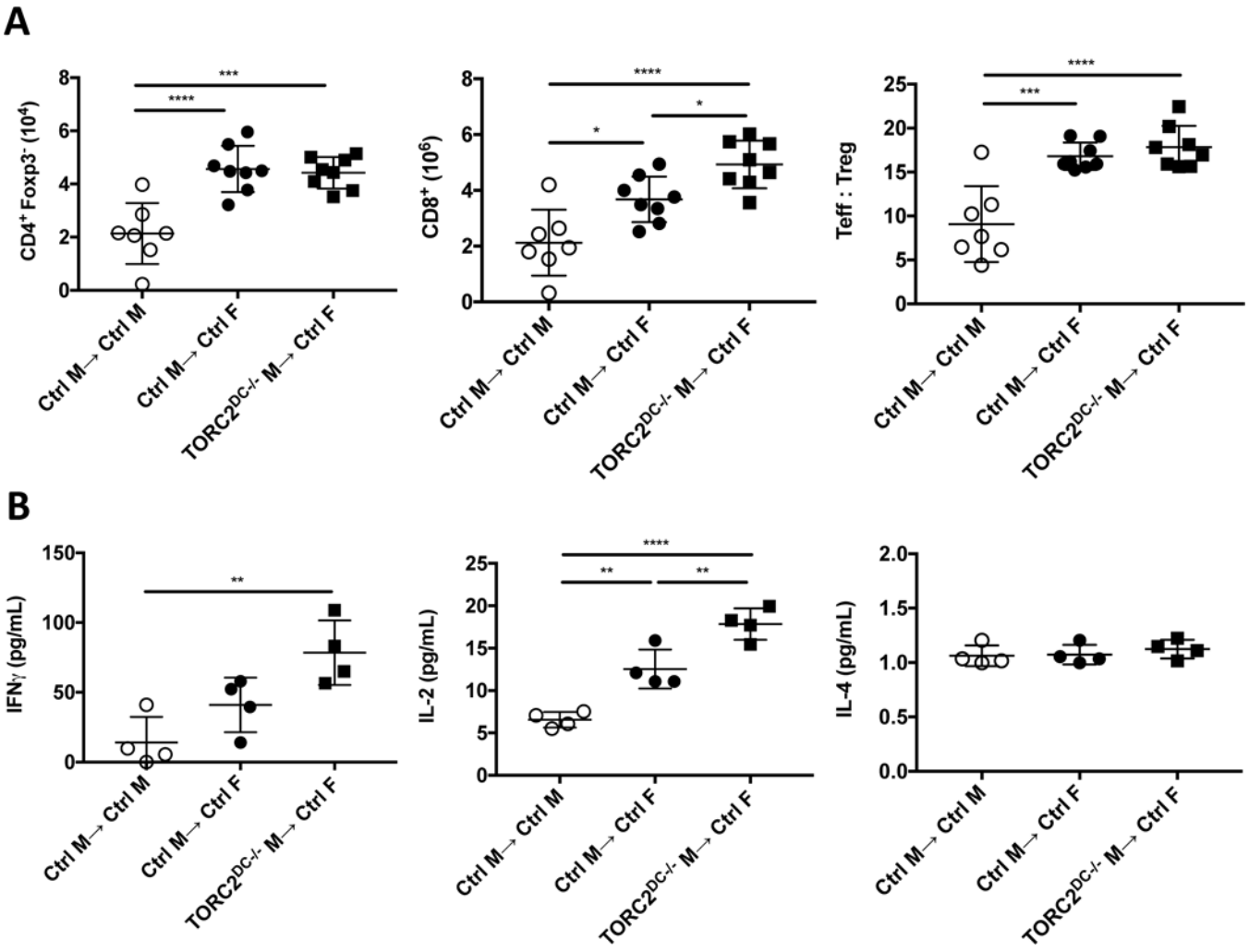

FIGURE 4.

HY-mismatched skin grafts from TORC2$^{DC-/-}$ male (M) donors elicit enhanced numbers of CD8$^+$ T cells in draining lymph nodes (LN) and augmented IFNγ and IL-2 production in response to donor Ag stimulation. T cells were isolated from the axillary LN of skin graft recipients on post-operative day 7. (A) Total numbers of CD4$^+$CD25$^-$Foxp3$^-$ T effector (Teff) cells, CD8$^+$ T cells and the ratio of Teff: Treg (CD4$^+$CD25$^+$Foxp3$^+$) cells. *n=8* mice per group; one-way ANOVA Tukey's multiple comparisons test, *, *p < 0.05;* ***, *p<0.001;* ****, *p<0.0001.* (B) Isolated T cells were co-cultured with splenic DCs isolated from Flt3L-mobilized male mice for 3 days. Levels of IFNγ, IL-2 and IL-4 in the supernatants. *n=4* mice per group; one-way ANOVA Tukey's multiple comparisons test*; **, p<0.01*; ****, *p<0.0001.*

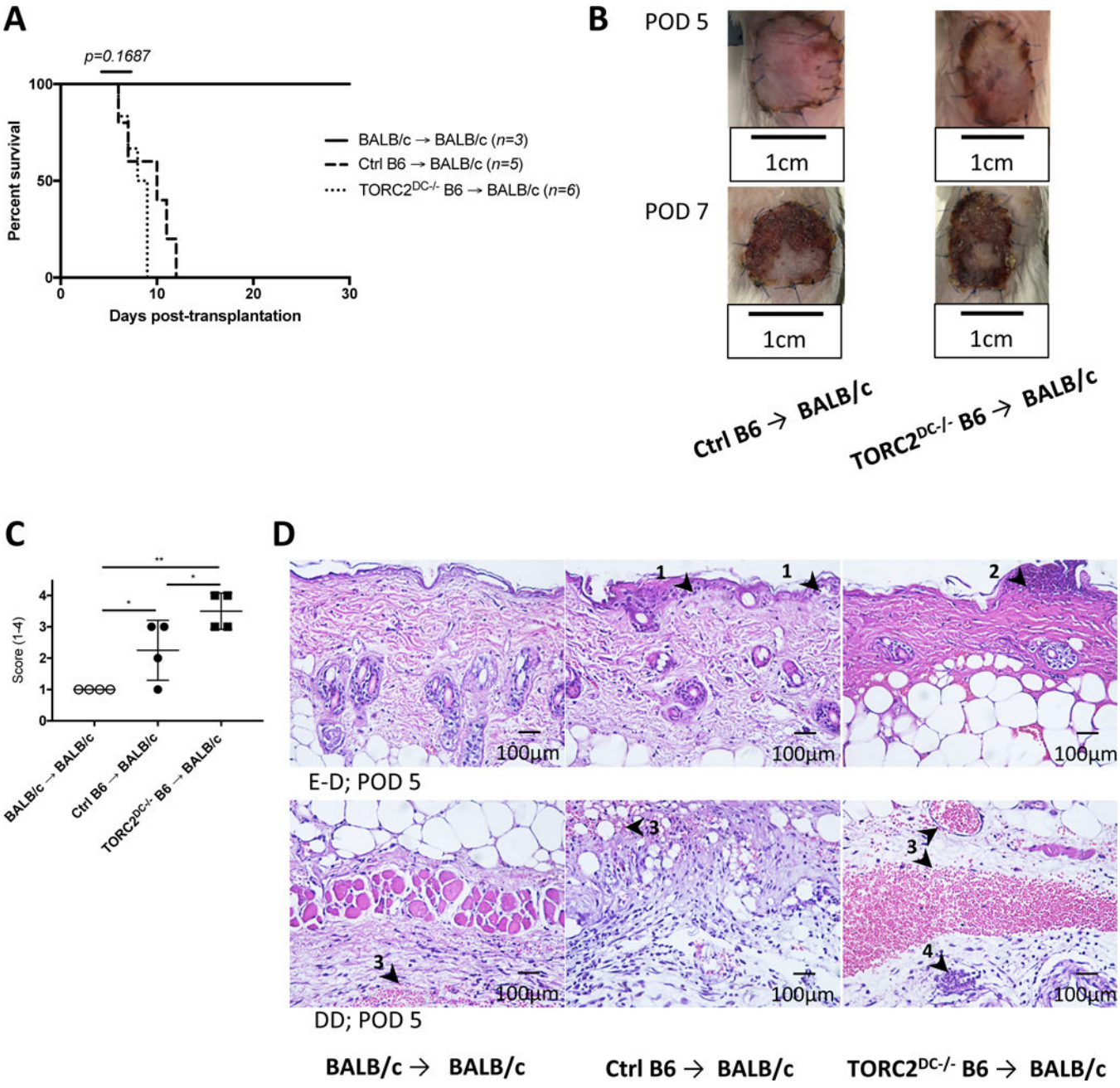

Figure 5.

MHC-mismatched skin grafts from TORC2$^{DC-/-}$ donors exhibit enhanced Banff rejection scores compared with grafts from Ctrl donors. Wild-type BALB/c mice received full-thickness skin grafts from either B6 WT control (Ctrl B6) or TORC2$^{DC-/-}$ B6 donors. (A) Graft survival over time; *n=3–6* mice per group; Log-rank test. (B) Representative gross morphology of skin grafts at post-operative day (POD) 5 and POD 7. (C) Banff rejection scores of skin grafts at POD 5; *n=4* mice per group; one-way ANOVA Tukey's multiple comparisons test; *, $p < 0.05$; **, $p < 0.01$. (D) Representative H&E staining of skin grafts at POD 5 showing (above) the epidermal-dermal junction (E-D) and (below) the deep dermal

layer (DD). Arrowheads indicate (1) vacuolar damage, (2) pathological diskeratosis, (3) thrombosis, and (4) vasculitis.

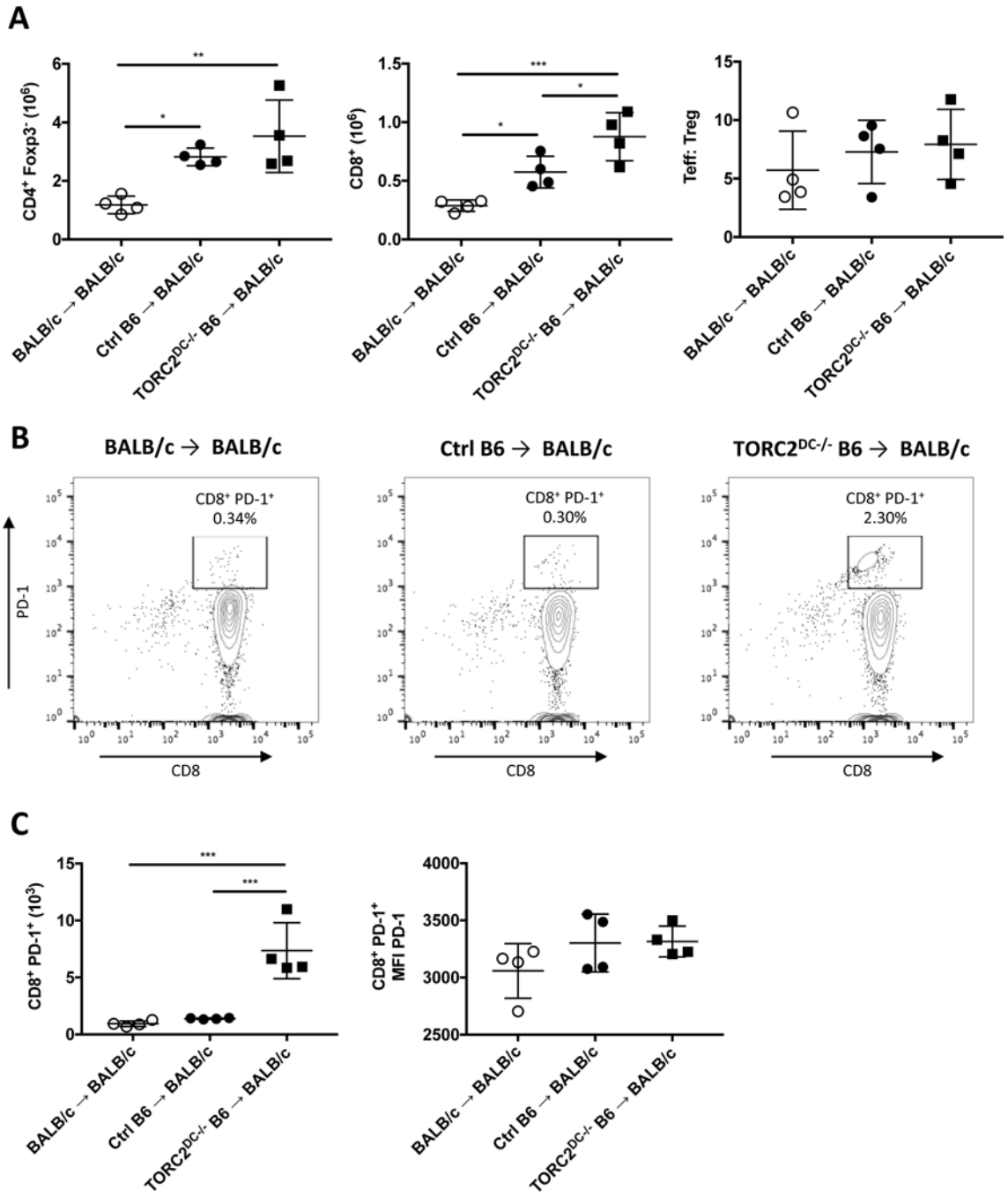

Figure 6.

MHC-mismatched skin grafts from TORC2$^{DC-/-}$ B6 donors elicit enhanced numbers of CD8$^+$ and CD8$^+$PD-1$^+$ T cells in draining lymph nodes (LN) of WT BALB/c recipients. T cells were isolated from the axillary LN of graft recipients on post-operative day 5. (A) Numbers of CD4$^+$CD25$^-$Foxp3$^-$ T effector (Teff) cells, CD8$^+$ T cells and the ratio of Teff: Treg (CD4$^+$CD25$^+$Foxp3$^+$) cells. (B) Representative histograms of CD8$^+$PD-1$^+$ T cells within LN of each group. (C) Numbers of CD8$^+$PD-1$^+$ T cells within LN (left) and MFI of

PD-1 on PD-1^{+} cells (right). *n=4* mice per group; one-way ANOVA Tukey's multiple comparisons test, *, *p < 0.05; **, p<0.01*, ***, *p<0.001*.

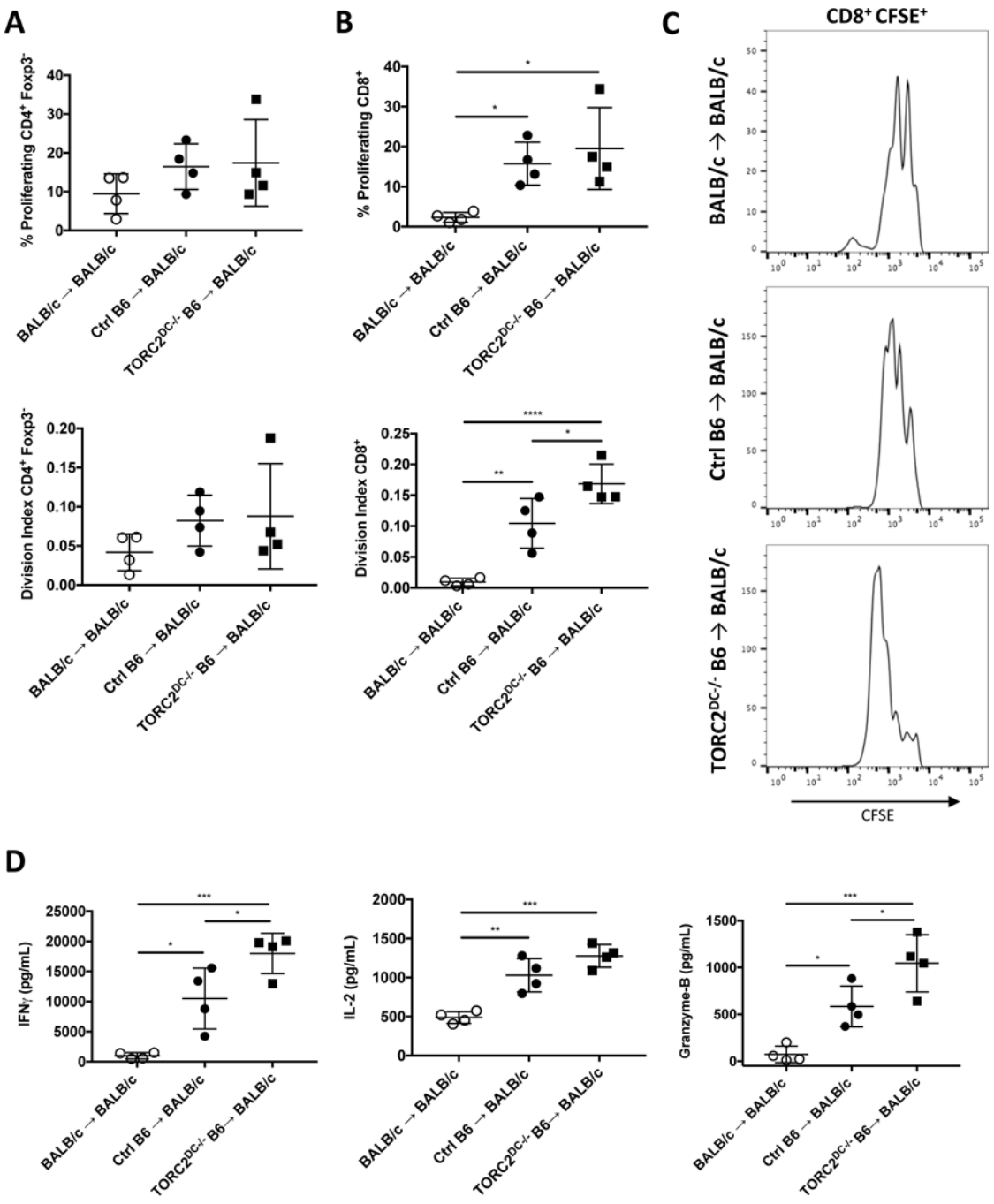

Figure 7.

MHC-mismatched skin grafts from TORC2$^{DC-/-}$ donors elicit enhanced proliferation of CD8^{+} T cells in draining lymph nodes (LN) and augmented IFNγ and IL-2 production in response to donor Ag stimulation. T cells were isolated from the axillary LN of TORC2$^{-/-}$ or WT control (Ctrl) skin graft recipients (BALB/c) on POD 5. Isolated T cells were labeled with the cell proliferation dye CFSE, and stimulated with B6 splenic DC for 3 days. (A) Proliferation of CD4^{+}Foxp3^{-} T cells measured by cellular CFSE content (above, percent dividing; below, division index). (B) Proliferation of CD8^{+} T cells as measured by cellular

CFSE content (above, percent dividing; below, division index). (C) Representative cell proliferation profiles from each group. (D) Levels of IFNγ, IL-2, and GrB in the culture supernatants. *n=4* mice per group; one-way ANOVA Tukey's multiple comparisons test, *, $p < 0.05$; **, $p<0.01$, ***, $p<0.001$, ****, $p<0.0001$.

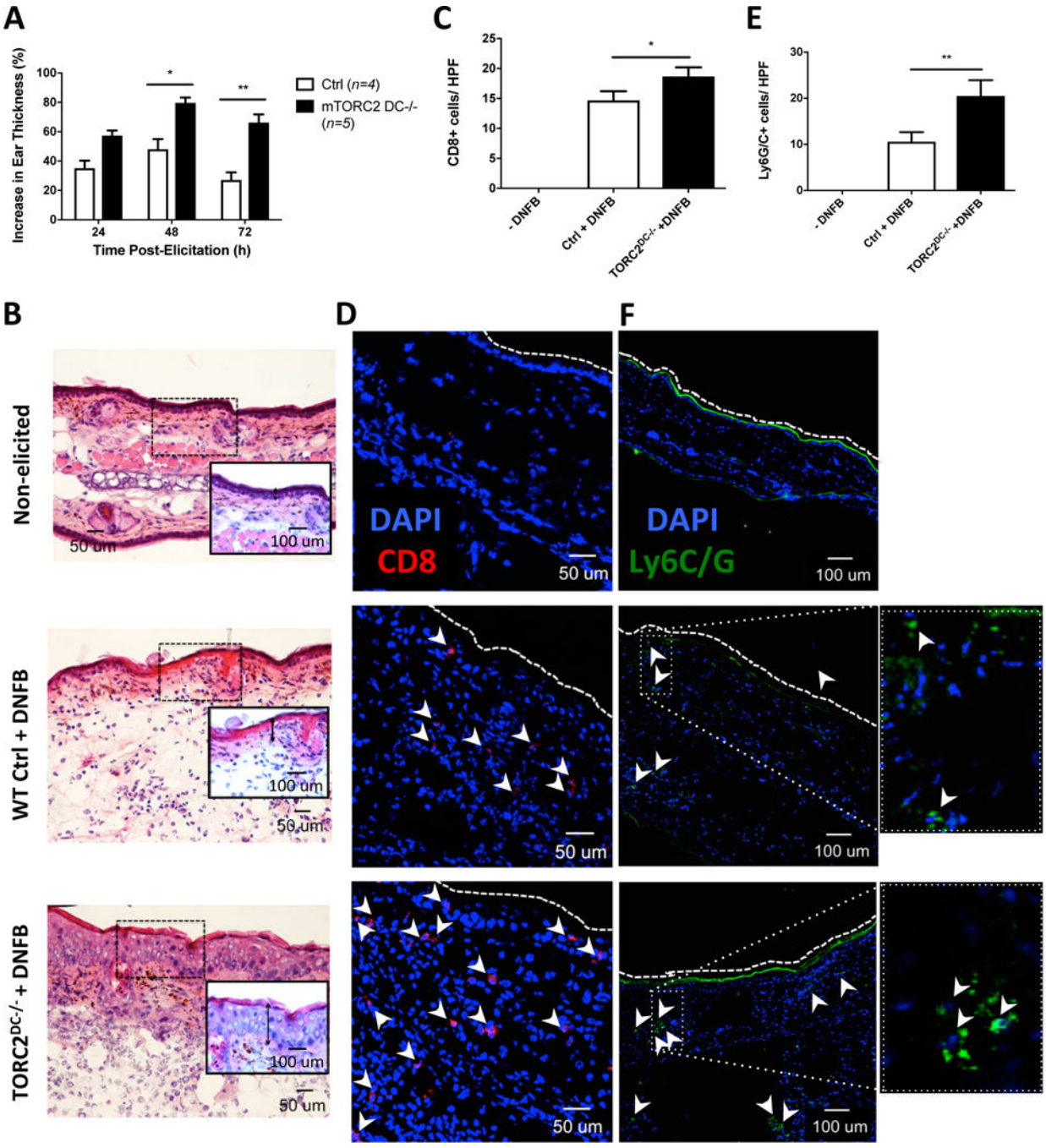

FIGURE 8.

TORC2$^{DC-/-}$ mice exhibit enhanced cutaneous delayed-type hypersensitivity (DTH) responses. Female WT control (Ctrl) or TORC2$^{DC-/-}$ mice were sensitized with dinitrofluorobenzene (DNFB) on the skin of the abdomen on day 0, then challenged 5 days later with DNFB on the right ear pinna to elicit a DTH response. (A) Percent increase in pinna thickness of the elicited ear compared with the non-elicited ear 24, 48, and 72 hours post-challenge; Student's t-test *, $p<0.05$; **, $p<0.01$. (B) Representative H&E staining of non-elicited and DNFB-challenged ears, as indicated; images are representative of *n=4–5*

mice. Insets are higher power views of the areas highlighted. Vertical inverted arrows indicate the thickness of the epidermal layer. (C) Numbers of $CD8^+$ cells within the ear pinna 72 hours post-challenge; *n=3* high-powered fields (HPF) per mouse; *4–5* mice per group; Student's t-test, *, $p < 0.05$. (D) Representative immunofluorescence (IF) DAPI (blue) and CD8 (red) staining (arrowheads) of non-elicited and challenged ears. (E) Numbers of $Ly6G/C^+$ cells within the ear pinna 72 hours post-challenge; *n=4–5* mice per group; Student's t-test, **, $p < 0.01$. (F) Representative IF DAPI (blue) and Ly6G/C (green; arrowheads) staining of non-elicited and challenged ears. Images on the far right are higher power views of the rectangular areas outlined by dotted lines in (F).

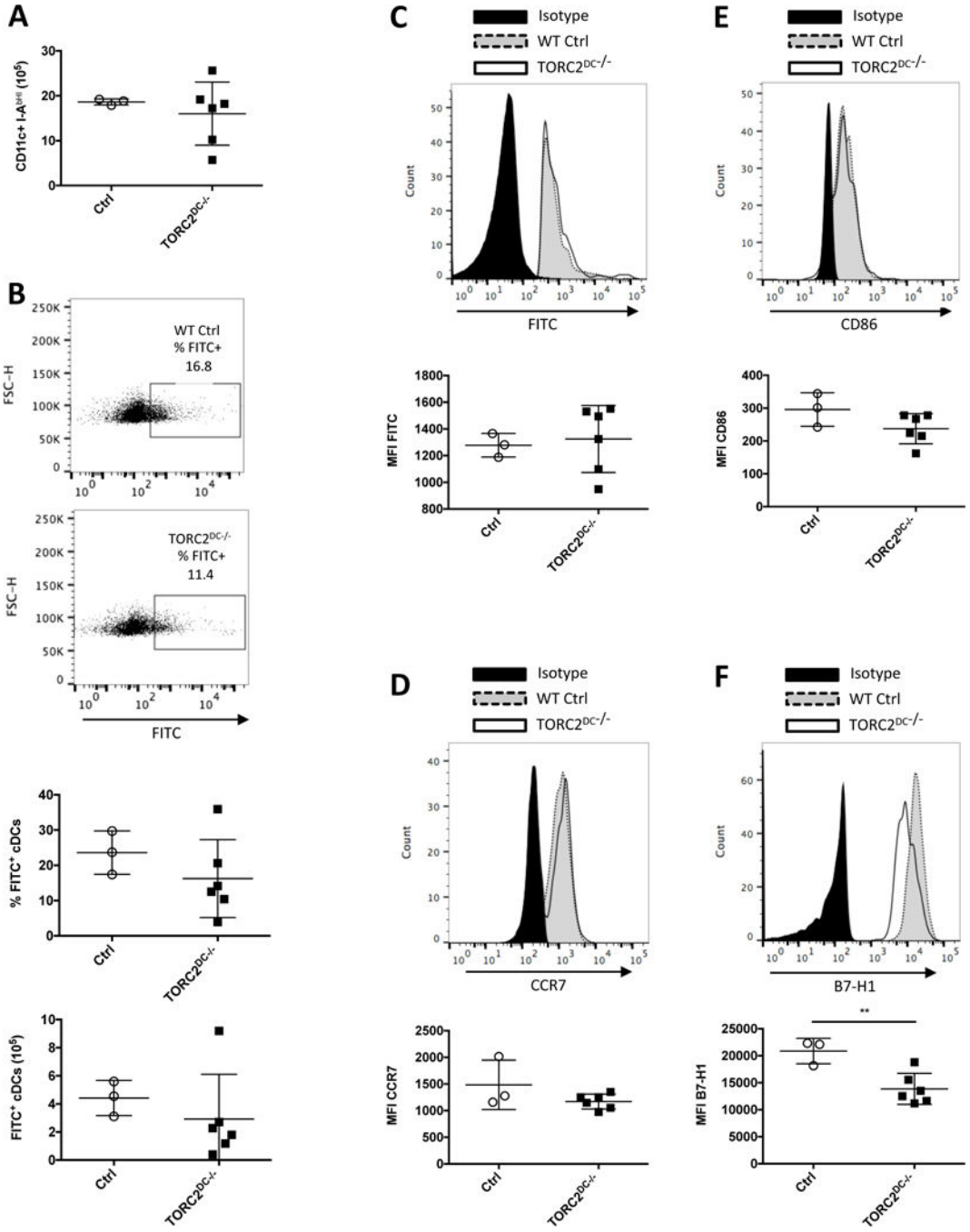

FIGURE 9.

TORC2$^{DC-/-}$ mice do not exhibit enhanced skin DC migration to regional lymph nodes (LN), but display reduced B7-H1 expression on DC compared with WT control (Ctrl) mice. WT Ctrl or TORC2$^{DC-/-}$ B6 mice were painted with FITC on the back of the ear pinna and cells were isolated from the cervical LN 24 hours later. (A) Numbers of (CD11c^{+}IA$^{b\ hi}$) DC in the LN. (B) Representative data (above) and incidence and absolute numbers (below) of FITC^{+} conventional DCs (CD11c^{+} I-A$^{b\ hi}$). (C) Above, representative flow profiles and below, mean fluorescence intensity (MFI) of FITC staining on FITC^{+} DC. (D) Above,

representative flow profiles and below, MFI of CCR7 staining on $FITC^+$ DC. (E) Above, representative flow profiles and below, MFI of CD86 staining on $FITC^+$ DC. (F) Above, representative flow cytometry and below, MFI of B7-H1 staining on $FITC^+$ DC in LN. *n=3–6* mice per group; Student's t-test, **, $p<0.01$.